The dipole moment of 18-crown-6: Molecular dynamics study of the structure and dynamics of the macrocycle in vacuo and in cyclohexane

ARTICLE *in* THE JOURNAL OF CHEMICAL PHYSICS · SEPTEMBER 1995

Impact Factor: 2.95 · DOI: 10.1063/1.470652

2 AUTHORS, INCLUDING:

Wim J Briels
University of Twente
178 PUBLICATIONS **4,355** CITATIONS

The dipole moment of 18-crown-6: Molecular dynamics study of the structure and dynamics of the macrocycle in vacuo and in cyclohexane

F. T. H. Leuwerink and W. J. Briels
Chemical Physics Laboratory, University of Twente, P.O. Box 217, 7500 AE Enschede, The Netherlands

(Received 14 February 1995; accepted 31 May 1995)

We have performed very long simulations of the 18-crown-6 molecule in the gas phase and in cyclohexane. For the isolated molecule we have used two different sets of charges. For all simulations the average dipole moment was in moderate agreement with experiment. Therefore we have examined in some detail the theoretical models used for the interpretation of the experiments. We propose a new formula, based on the Kirkwood equation, to calculate the molecular dipole moment from the experimental dielectric constants. With previously published experimental data, we have calculated a dipole moment that is somewhat larger than the originally reported value. We conclude that the charges that have been used in all potential models up to now may, at best, be treated as effective charges and that polarization is expected to be important. We made an extensive investigation of the structure of 18-crown-6 during the simulations. It was observed that conformational statistics was almost the same *in vacuo* and in the apolar cyclohexane. The structure of the crown ether is found to fluctuate around the centrosymmetric C_i conformation. A comparison is made with previously published statistical mechanical studies. We also examined the average shape of 18-crown-6 by looking at the mass distribution within the molecule. Again it was found that the crown ether, on average, displays an elliptical shape, consistent with the other results. Further, it was found that many of the samples show the same structural features, although they do not exhibit the same conformation. Finally, the dynamics of the different systems was investigated. As expected, it has been found that the solvent slows down the dynamics of the crown ether molecule. © *1995 American Institute of Physics.*

I. INTRODUCTION

Since their discovery by Pedersen in 1967,[1] macrocyclic polyethers have been the subject of numerous studies of diverse character. Their remarkable complexing power has led to considerable interest in the conformations these molecules can adopt. An enormous amount of x-ray crystallographic data has been obtained over the years, yielding structural information of numerous complexes with cations and organic molecules.

Besides the experimental information from x-ray studies,[2–4] spectroscopic studies[5–7] etc., an increasing amount of detailed information has been obtained by the application of computational methods to study the properties of macrocyclic polyethers. For many of these theoretical studies, one of the simplest flexible polyethers, the prototypical crown ether 1,4,7,10,13,16-hexaoxacyclooctadecane (18-crown-6), has been used. Semiemperical and *ab initio* calculations have been carried out by Yamabe *et al.*,[8] Hori *et al.*,[9] and Bruning and Feil[10] to examine electronic and complexation properties. Wipff *et al.*[11] performed a molecular mechanics study on the structural flexibility of 18-crown-6. They minimized the energy of different structures. In an environment with a low dielectric constant the lowest-energy structure had the same conformation (C_i symmetry) as that found in the crystal structure of uncomplexed 18-crown-6. In a more polar environment the D_3d conformation becomes more stable. Wipff and co-workers also predicted the existence of a C_1' conformation that could explain the temperature-dependent dipole moment of 18-crown-6. Since then, several authors have extended such investigations.[12–14]

Because the aim of conformational analysis is to find the thermally populated conformations of a molecule, and, because of the importance of interactions with a surrounding solvent, interest has shifted toward techniques like molecular dynamics and the Monte Carlo method. Sun and Kollman,[15] for instance, determined the solvation free energy for a number of conformations of 18-crown-6, and found that in water the D_3d structure is the most stable one. Straatsma and McCammon[16] sampled and discussed numerous conformations of the crown ether molecule in aqueous solution in their article on the treatment of rotational isomers in free energy calculations. Sun and Kollman[17] used 18-crown-6 as a test case for conformational sampling and ensemble generation by molecular dynamics simulations. Leuwerink *et al.*[18] simulated different complexes of 18-crown-6 and compared conformational data from these simulations with information from the Cambridge Structural Database. From all these studies it is clear that 18-crown-6 is a highly flexible molecule that can adopt many different conformations lying within a narrow energy range. The complexing power of crown ethers and their role as a catalyst[19,20] can be related to this flexibility, giving them the possibility to adopt a conformation exhibiting a reaction site toward a given reagent.

Experimental work on the dipole moment suggests that the conformations adopted by 18-crown-6 are quite variable, depending on the environment and the thermodynamic conditions. Perrin *et al.*,[21] who measured the dipole moment of liquid 18-crown-6, found that it increases with temperature in the range 50 °C–100 °C, leading to the conclusion that the molecule adopts various conformations that are close in energy and have very different dipole moments, and that the

populations of these conformations are temperature dependent. Caswell and Suvannunt[22] measured the dipole moment of several crown ethers in both benzene and cyclohexane at different temperatures, and found a temperature-dependent dipole moment as well. As in the investigation of Perrin *et al.*, the values of the dipole moment reported by Caswell and Suvannunt clearly show that the uncomplexed 18-crown-6 does not exhibit the same conformations in solution and in the solid state. Both groups also presented a seminal molecular mechanics study. For a limited number of conformations, taken from crystallographic data and extended with few hypothetical ones, the relative energies and dipole moments were calculated. Again, it was found that the crown is capable of adopting conformations with very different dipole moments, that are close in energy. A more extensive theoretical investigation that closely links up with the experimental work mentioned above, is the Monte Carlo study of Ha and Chakraborty[23] on the effect of solvent polarity and temperature on the conformational statistics of 18-crown-6. They concluded that temperature and solvent polarity have a large influence on the crown's structure. Although many conformations are populated, the D_3d structure appears to be the dominant conformation in water and the C_i conformation is the dominant form in a CCl_4 solution. Like Perrin *et al.*, Ha and Chakraborty, too, provided a dipole moment that reflects the presence of many different conformations in solution, but which is in moderate agreement with experiment.

In this paper we study the conformational characteristics of 18-crown-6, both static and dynamic, and both *in vacuo* and in cyclohexane. To this end we have performed several molecular dynamics simulations, the computational details of which are described in Sec. II. In Sec. III A and III B we describe the statistics of the molecular dipole, while in Sec. III C we look at the distribution of the mass within the molecule. In Sec. IV we present the derivation of an expression relating the dielectric constant of dilute solutions of polar molecules to the molecular dipoles. We use this formula to calculate the molecular dipole moment from the experimental data of Caswell and Suvannunt.[22] In Sec. V we study the dynamical properties of 18-crown-6. In the final Sec. VI, we present the conclusions.

II. COMPUTATIONAL DETAILS

The molecular dynamics simulations described in this paper were performed using the simulation package GROMOS.[24]

Several simulations have been performed: simulations of 18-crown-6 in vacuum; a simulation of the crown in cyclohexane; and simulations of pure cyclohexane and of liquid 18-crown-6. The simulation of cyclohexane was done in order to calculate, in combination with data from the solution, the partial molar volume of the crown ether molecule in cyclohexane (see Sec. IV B). The liquid 18-crown-6 simulation was done to see whether the experimental density could be reproduced with the force field used to model the crown. This, to check if the partial molar volume of 18-crown-6 in cyclohexane is no artefact of the force field. In all simulations described below, the starting structure of the crown ether molecule was chosen to be the D_3d conformation.

The simulation of the isolated 18-crown-6 molecule was done in the NVE ensemble. The SHAKE procedure[25] was applied to constrain all the hydrogen–carbon bond lengths. Every 500 ps, the energy was carefully adjusted until the desired temperature of 298 K was reached. Then, the system was equilibrated for another 500 ps. Next, a large number of consecutive runs were performed, each with a length of 1 ns. The molecule was simulated for a total of 30 ns. The fluctuations in the temperature amounted to approximately 30 K.

Two simulations of the isolated molecule were done, employing two different potential models; we will refer to these simulations as *in vacuo* simulation I and *in vacuo* simulation II. The second simulation was performed in order to investigate the effect of different sets of charges on the dipole moment. The computational details were the same as for *in vacuo* simulation I, but the total length amounted to 15 ns.

The solution of the crown ether in cyclohexane, the pure solvent, and the liquid 18-crown-6 were all simulated in the NpT ensemble. The temperature and pressure were maintained at ambient values by scaling, respectively, the velocities with a coupling time constant of 0.1 ps, and the coordinates with a time constant of 0.5 ps.[26] All bonds were kept at their equilibrium lengths using the SHAKE coordinate resetting procedure. Two starting configurations were prepared for the solution. Both systems were equilibrated for 250 ps, followed by a production run of 1 ns.

The cyclohexane was simulated for 150 ps after an equilibration of 250 ps. The average volume observed leads to a density of 0.787 g/cm^3. This is slightly higher than the experimental value 0.774 g/cm^3 (298 K).[27]

Because of the crown's vast configuration space, and because of the fact that the sampled section of the configuration space is correlated with the starting conformation, the system for the liquid 18-crown-6 simulation was heated up first and simulated for 25 ps at 600 K. Next, it was cooled down stepwise in a total of seven intermediate runs, all with a length of 10 ps. The jumps in the temperature during the cooling process were gradually made smaller in the vicinity of the final temperature of 323 K. At 323 K the system was equilibrated for an extra 30 ps. The density of 1.041 g/cm^3 calculated from the production run is 4.5% lower than the experimental value 1.090 g/cm^3 (323 K).[21] In all the simulations, a time step of 0.002 ps was used. A complete survey of the simulation details can be found in Table I.

The molecular interactions were described using the energy expression

$$V_{\mathrm{pot}} = \sum_{\mathrm{bonds}} \frac{1}{2} k_b (b - b_0)^2 + \sum_{\mathrm{angles}} \frac{1}{2} k_\theta (\theta - \theta_0)^2 + \sum_{\mathrm{dihedrals}} \frac{1}{2} V_n \{1 + \cos(n\omega - \delta)\} + \sum_{\mathrm{nonbonded}} \left(\frac{C_{12ij}}{r_{ij}^{12}} - \frac{C_{6ij}}{r_{ij}^{6}} + \frac{q_i q_j}{4\pi\epsilon_0 r} \right). \quad (1)$$

The parameters for the 18-crown-6 molecule were taken from the AMBER all-atom force field,[28] with a 50% scaling for the 1–4 van der Waals interactions. For *in vacuo* simulation I, the solution and the liquid 18-crown-6, the atomic

TABLE I. Summary of simulation details.

	Vacuum I	Vacuum II	Solution	Cyclohexane	Liquid 18C6
Number of 18-crown-6 molecules	1	1	1	⋯	125
Number of cyclohexane molecules	⋯	⋯	225	216	⋯
Ensemble	NVE	NVE	NpT	NpT	NpT
Simulation time (ps)	30 000	15 000	2000	150	50
Periodic boundary	⋯	⋯	truncated octahedron	cubic	cubic
Cutoff radius (Å)	…[a]	…[a]	10	14	12.5
τ_T (ps)	⋯	⋯	0.1	0.1	0.1
τ_p (ps)	⋯	⋯	0.5	0.5	0.5
Storage coordinates, etc. (ps)	0.1	0.1	0.1	0.02	0.02
Update pairlists (ps)	0.8	0.8	0.02	0.02	0.02
Density (g/cm^3)	⋯	⋯	⋯	0.787[b]	1.041[c]
Reference pressure (atm)	⋯	⋯	1	1	1
Average temperature (K)	297	300	299	299	322

[a]> dimensions molecule.
[b]Experimental value: 0.744 g/cm^3 (Ref. 27).
[c]Experimental value: 1.090 g/cm^3 (Ref. 21).

charges for the crown ether ($q_O=-0.30e$) were taken from the molecular mechanics study of Wipff *et al.*[11] For *in vacuo* simulation II the charges for the 18-crown-6 molecule ($q_O=-0.406e$) were derived from *ab initio* electrostatic potential calculations.[29]

Each methylene unit in a cyclohexane molecule was treated as a single force center with appropriate mass. The parameters for this solvent molecule were taken from Harris and Stillinger,[30] who studied the liquid structure of cyclohexane. The parameters of their revised Lennard-Jones and torsional contribution, were adapted to the form of the potential energy function of GROMOS.

The computational boxes of the solution and the pure solvent were prepared with all cyclohexane molecules in the chair conformation. Calculation has shown that the twisted boat isomer lies 28.6 kJ/mol (expt.: 23 kJ/mol) in energy above the chair minimum.[30]

III. CONFORMATIONAL ANALYSIS

In this section we describe structural aspects of the 18-crown-6 molecules from the different MD runs in relation to their dipole moments. It is to be expected that the distribution of its conformations is rather similar in vacuum and in the solution.

A. Conformational sampling and dipole moment statistics

The production run of the solution altogether lasted 2 ns. During this simulation, numerous dihedral transitions were observed. The total number of symmetry-unique conformations amounted to 408. Like in the case of the study of Straatsma and McCammon,[16] who performed a long MD run of an aqueous solution of 18-crown-6, the simulation described here was still generating new conformations after 2 ns, and the generated ensemble will therefore not be completely representative for the Hamiltonian used. In contrast to the crown ether, no dihedral transitions were observed for the solvent. All cyclohexane molecules stayed in the chair conformation during the entire simulation.

During *in vacuo* simulations I and II, a total of, respectively, 5628 and 3568 symmetry-independent conformations were sampled, and, as in the case of the solution, new conformations appeared continuously along the trajectory, and no convergence was obtained. (Notice that simulation I was twice as long as simulation II.) In both cases, the C_i conformation was most frequently sampled (resp., 5.90% and 10.67%), in accordance with previous studies on this subject.[11,17,18] The D_3d conformation only appeared during simulation I (1.18%; number eight in the frequency list). Conformations with an occurrence of 0.5% or more (30 and 35 in total with, respectively, potential models I and II) contributed to 34.73% and 40.68% of the total population.

The C_i and D_3d structures were not sampled in the cyclohexane solution. The conformation with the highest frequency in solution (10.18%) was a structure with a nonzero dipole moment, and had C_1 symmetry. The 36 conformations with an occurrence of 0.5% or more, constituted 73.49% of the total.

The centrosymmetric C_i and D_3d conformations are all but the only two structures found in crystals. It is well established that when crystallized from apolar, aprotic solvents, 18-crown-6 adopts the C_i conformation.[31,32] The D_3d arrangement is observed in crystals with metal ions, as well as in complexes where the crown is surrounded by polar O–H, C–H, or N–H bonds.[33–35] NMR studies in solution suggest that the conformation of the uncomplexed crown is the same in apolar solvents as in the solid phase,[7] but other conformations should be expected in polar media.[6]

Figure 1 gives the distributions of the crown ether dipole moments for, respectively, *in vacuo* simulation I (top), the cyclohexane solution (middle), and *in vacuo* simulation II (bottom). Corresponding averages are given in Table II. The distributions of gas phase simulation I and the solution are almost identical. Both have a maximum at approximately 1.8 D. The statistics of gas phase simulation II is very different. Here we see two peaks, at 0.8 and 2.5 D. With this force field, the conformations are distributed more irregularly then in the other two calculations, which manifests itself in an average dipole moment of 2.39 D, which is smaller than

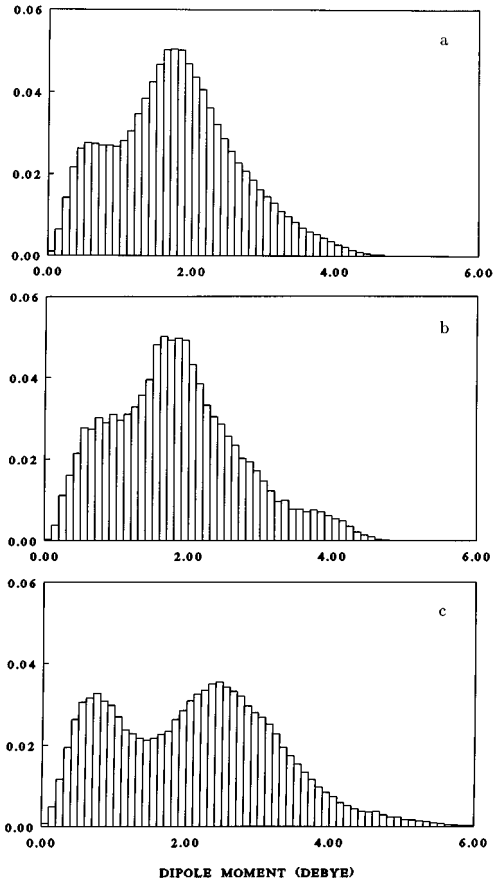

FIG. 1. Normalized distributions of the dipole moment of 18-crown-6: (a) *in vacuo* simulation I; (b) cyclohexane solution; (c) *in vacuo* simulation II.

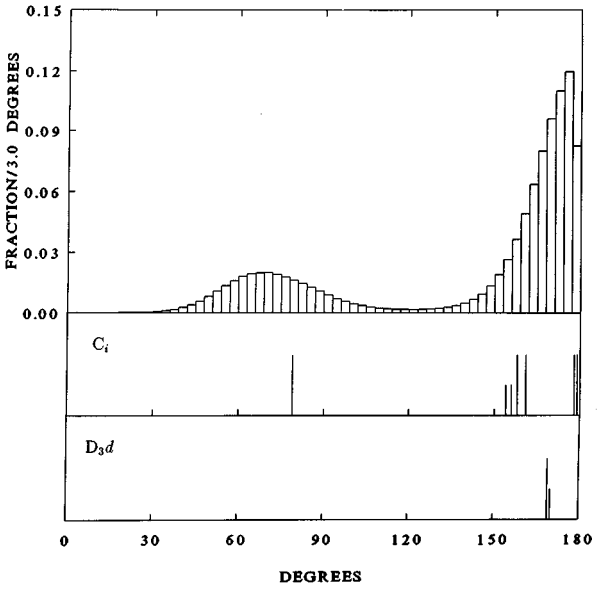

FIG. 2. CO–CC torsion angle distribution from *in vacuo* simulation I (top), for the minimal energy C_i conformation (middle), and the minimal energy D_3d conformation (bottom).

expected on account of the difference between the sets of charges alone. Recently, an MD study was published by Troxler and Wipff,[36] in which the conformations and dynamics of 18-crown-6 in acetonitrile were studied. They used nearly the same potential model for the macrocycle we used in *in vacuo* simulation II. The distribution of the dipole moments presented by Troxler and Wipff (Fig. 6 of Ref. 36) shows the same characteristics as the one presented here [Fig. 1(c)]. They also observed two maxima, but the second peak is found at a considerable lower value. Further, they found the D_3d and the C_i conformations to be the structures with the largest occurrence. Ha and Chakraborty,[23] who used a united atom force field with $q_O=-0.30e$, reported an average dipole moment of 1.92 D at 298 K in CCl_4, which should be compared with the value of 2.04 D we obtained from the solution (see Table II). Troxler and Wipff reported an average dipole moment of 2.1 D (with a mean square deviation of 1.2 D). They state that if q_O charges of $-0.30e$ had been used, this would have lead to a dipole moment of 1.6 D, which is significantly lower than our result, and the result of Ha and Chakraborty. We note that the reported values of the dipole moments are quite different from that (0.8 D) calculated by Wipff *et al.*[11]

B. Statistics of the dihedral angles

Apparently the statistics of the crown ether is the same in the apolar solvent and for the isolated molecule. To elaborate on this, conformational statistics of the macrocycle was characterized via the distributions of the CO–CC and OC–CO torsion angles. The distributions for *in vacuo* calculation I are shown in Figs. 2 and 3, together with the molecular mechanics predictions for the centrosymmetric C_i and D_3d structures as δ functions. Only the results for the gas phase are shown, because those of the solution were found to be only marginally different.

We also examined the statistics of the torsion angles for *in vacuo* simulation II. The distributions (not shown here) display the same features as for the other two runs: both the

TABLE II. Average dipole moments calculated from the simulations (in Debye).[a]

	$\langle\mu_x\rangle$	$\langle\mu_y\rangle$	$\langle\mu_z\rangle$	$\langle\mu^2\rangle^{1/2}$
In vacuo simulation I	−0.0022(0.2801)	0.0455(0.2787)	−0.0225(0.3668)	1.98(0.22)
In vacuo simulation II	−0.1577(0.3829)	−0.0783(0.4127)	−0.1258(0.2716)	2.39(0.25)
Cyclohexane solution	−0.0017(0.7481)	0.0893(0.8107)	−0.1105(0.7098)	2.04(0.60)

[a]Standard deviations are given in brackets.

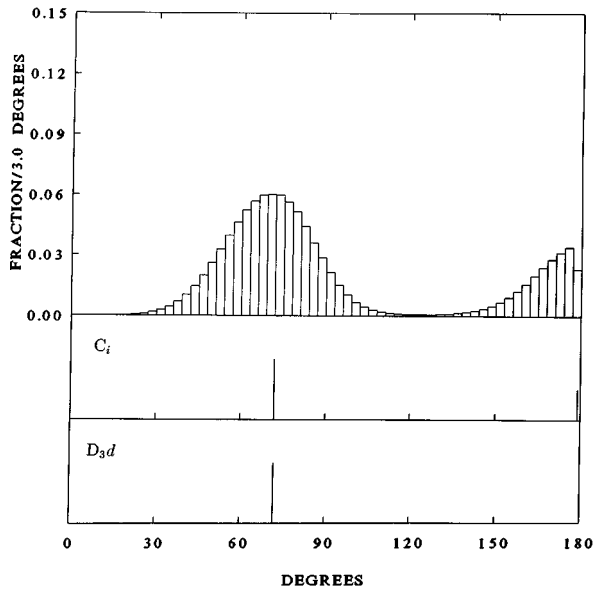

FIG. 3. OC–CO torsion angle distribution from *in vacuo* simulation I (top), for the minimal energy C_i conformation (middle), and the minimal energy D_3d conformation (bottom).

CO–CC and OC–CO dihedral angles peak for the gauche and trans conformations. But there are also some discrepancies. With the charges used in this simulation, slightly fewer dihedral angles are found in the trans conformation than for the other calculations, and slightly more in the gauche form. For gas phase simulation I and the simulation of the crown ether in cyclohexane, the maxima of the distributions of both types of dihedral angles are found at 70°. For gas phase simulation II these are found at 76° and 67°, for, respectively, the CO–CC and OC–CO type of torsion angles. Again we see an effect on the distribution of conformations with this force field, compared to the other two MD simulations. In Sec. III A we already noticed that the average dipole moment is smaller than to be expected on the basis of the difference between the sets of charges.

Like Ha and Chakraborty conclude for the crown in carbon tetrachloride, we too find, that for the cyclohexane solution, as well as for the isolated molecule, the average 18-crown-6 structure is close to the C_i conformation. However, many other conformations are also populated, which is also clear from the calculated average dipole moment. The distribution of the dihedral angles presented by Troxler and Wipff suggests that in acetonitrile the distribution is intermediate to those obtained by Ha and Chakraborty for the solvents water and CCl_4.

The solvent seems to have only an effect on the dynamics of 18-crown-6, which will be discussed in Sec. V, but not on the distribution of its conformations. This is different for a highly polar solvent like water. Ha and Chakraborty have shown that the distribution of the torsion angles in water is quite different from that in CCl_4. They come to the conclusion that in water the structure fluctuates around the crystallographic D_3d conformation. (The D_3d conformation is very often observed in x-ray structures of 18-crown-6 with metal ions or small organic molecules.) Further, they have shown, on the basis of radial distribution functions, that water molecules structure themselves around the crown ether molecule, by means of hydrogen-bonding interactions, which is quite different from that in carbon tetrachloride. These kind of interactions of water with the macrocycle, which have been observed in other studies as well,[37–39] tend to stabilize certain conformations. Straatsma and McCammon,[16] for example, found from their MD simulation of an aqueous solution of 18-crown-6, that the most populated conformations are of D_3d and C_1 symmetry. They pointed out that the solvent plays an important role in the stabilization of certain structures. A recent Raman spectroscopic study on the conformational equilibrium in water,[40] confirmed this D_3d predomination. So, statistics of the crown ether molecule is strongly influenced by these kind of solvents, compared to the free molecule or a solution in a nonpolar solvent.

C. Characterization of the structure of 18-crown-6 by means of the inertia tensor

Apart from the distribution of the dihedral angles, we have also studied the conformations and average shape of 18-crown-6 by examining the distribution of the mass within the molecule. This was done by calculating, for every sample, the inertia tensor:

$$I_{\alpha\beta} = -\sum_i m_i r_{i\alpha} r_{i\beta} + \delta_{\alpha\beta} \sum_i m_i r_i^2, \tag{2}$$

and next diagonalizing this tensor. The resulting eigenvectors were ranged in such a way that the x axis corresponds with the smallest principal moment of inertia, and the z axis corresponds with the largest principal moment of inertia. Notice that with the smallest principal moment corresponds the longest molecular axis, and with the largest principle moment the shortest molecular axis. Next, the mass distribution of every sample was described in its own principal axes coordinate system. In the following figures we present the densities obtained by projecting the atoms on the xy and xz planes, respectively. The contour plots in the yz plane are not shown. No new information results from these projections.

In Figs. 4(a)–4(d) the contour plots for oxygen and carbon in the xy and xz planes are shown. The plots relate to vacuum simulation I. From this figure we see immediately that the average shape of the molecule resembles that of a flattened ellipsoid. This is in accordance with the fact that from the distribution of the torsion angles the conformation of the molecule was found to fluctuate around the C_i conformation, which has an elliptical shape. Besides the average shape we recognize, from the projections on the xy plane, a pronounced structure in the distribution of the oxygen and carbon atoms. In the case of carbon, some atoms appear to be rather localized [left and right side of Fig. 4(b)], while others possess a large degree of freedom (top and bottom of the same figure).

Looking at the oxygen distribution, we expect a strong correlation between the different localized peaks. To investigate this, the coordinate sets that have one oxygen atom projected in the window in the lower right corner of Fig. 4(a), were separated from the rest. 25.7% of the samples satisfied

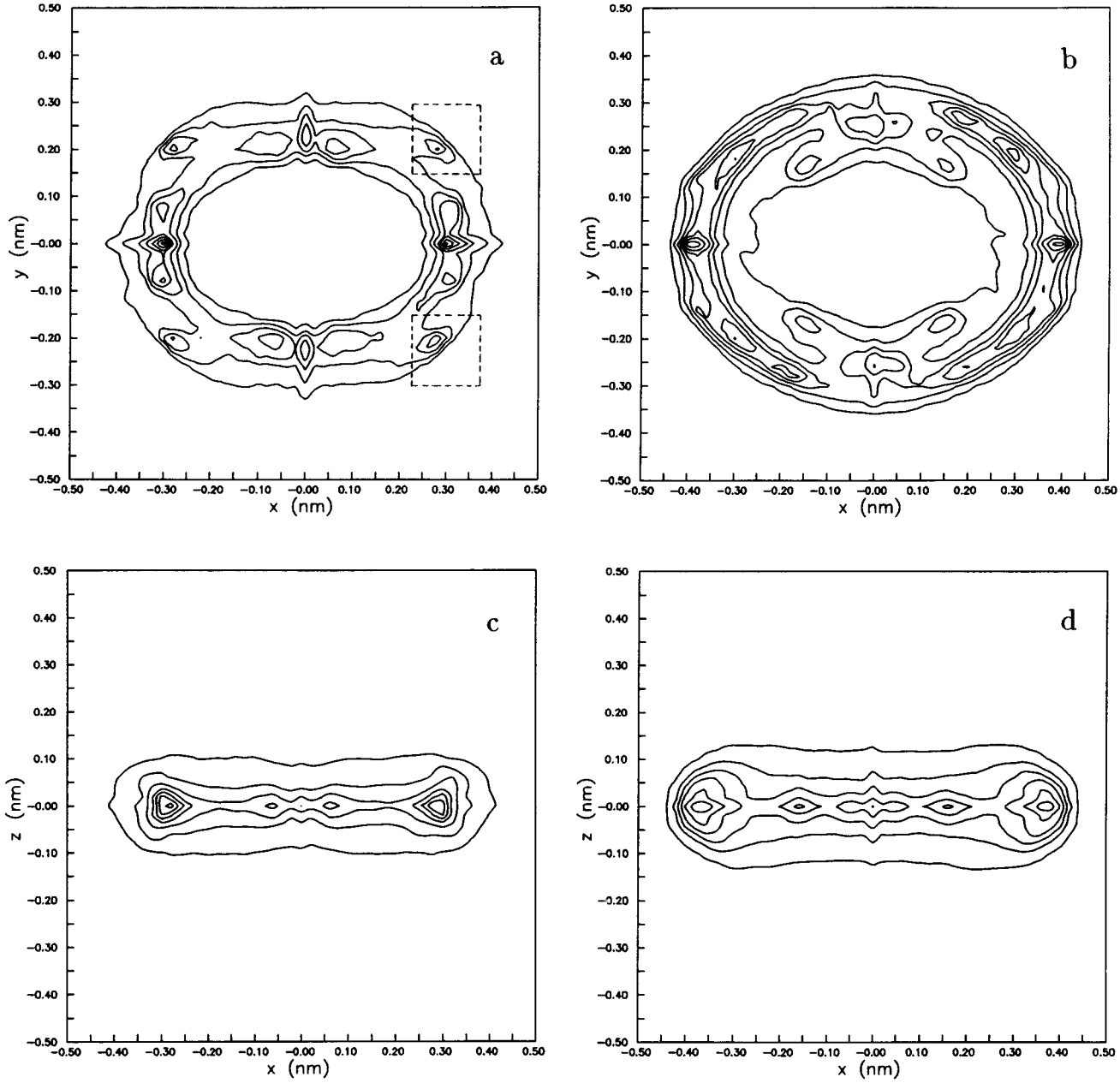

FIG. 4. Contour plots for *in vacuo* simulation I. (a) Projection of the oxygen atoms of 18-crown-6 on the *xy* plane; (b) projection of the carbon atoms of 18-crown-6 on the *xy* plane; (c) projection of the oxygen atoms on the *xz* plane; (d) projection of the carbon atoms on the *xz* plane. For these four plots, all samples were used that were recorded during the MD simulation.

this condition. The oxygen densities of this group of samples (group IA) are shown in Fig. 5, together with the corresponding carbon densities. The same was done for the coordinate sets, which have an oxygen atom projected in the window in the upper right corner of Fig. 4(a). 23.3% of the samples were found to constitute this group (group IB). The contour plots for this group are not shown. They are symmetry related to those of group IA by a counterclockwise rotation over 90°.

The distributions of these selections should be compared with the corresponding results for the optimized C_i and D_3d structures, which are shown in Fig. 9. The positions of the oxygens of the C_i conformation coincidence with the contour maxima in Fig. 5(a). Apparently, the samples of group IA are close to the C_i conformation. This is confirmed by the fact that the average principal moments of inertia for group IA closely resemble those of the minimized C_i conformation (Table III). From Table III we also see that the average moments of inertia for group IB are virtually the same as for group IA.

Next, groups IA and IB were removed from the total of samples. The remaining samples (group II) constitute 51.9% of the total. Notice that that this implies that 0.9% of all samples has one oxygen atom projected in the upper window

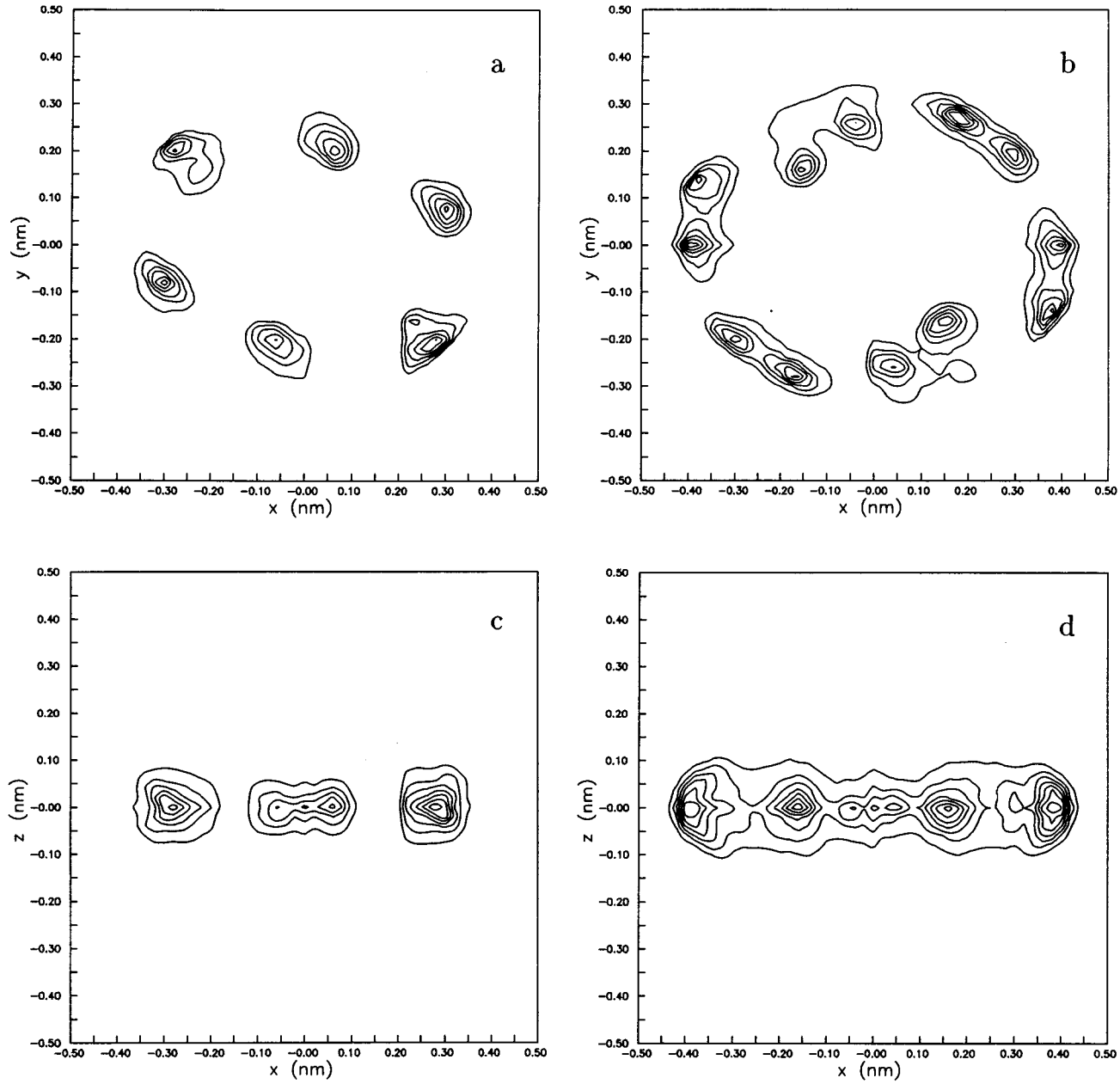

FIG. 5. Contour plots for *in vacuo* simulation I. (a) Projection of the oxygen atoms of the samples of group IA (see the text) on the *xy* plane; (b) projection of the corresponding carbon atoms on the *xy* plane; (c) projection of the oxygens of (a) on the *xz* plane; (d) projection of the carbons of (b) on the *xz* plane.

in Fig. 4(a), and at the same time another oxygen atom in the lower window of that same figure. The distribution of the samples of group II is shown in Fig. 6. Again, the six oxygens can clearly be distinguished. Moreover, the oxygen on the left and the oxygen on the right seem to be more localized than the other four. This feature matches with the fact that the corresponding carbon atoms [Fig. 6(b)] involved in the OC–CO dihedral angles with the neighboring oxygen atoms are quite fixed as well. The molecule seems somehow to be twisted around the remaining two OC–CO torsion angles [top and bottom of Fig. 6(b)]. Finally, group II is split up into two subgroups (IIIA and IIIB). All samples that have a projection in the window, as indicated in Fig. 6(a), are separated from the rest. The projections of the oxygens of the two subgroups in the *xy* and *xz* plane are shown in Fig. 7. Groups IIIA and IIIB, respectively, contain 39.6% and 12.3% of the total of samples.

In Table III also, the average moments of inertia of groups II and III are presented. The first impression from the contour plots of these remaining samples (Figs. 6 and 7) is that they are more symmetric, and perhaps closer to the D_3d [see Fig. 9(b)], than to the C_i structure. From Table III, however, we see that these samples are yet closer to the C_i than to the D_3d conformation. Although the two shorter axes differ less than in the case of groups IA and IB, the average shape of the molecule is still elongated.

TABLE III. Average principal moments of inertia ($*10^{45}$ kg m^2) for the different groups of coordinate samples (Sec. III C).[a]

In vacuo simulation I	C_i	D_3d	Group IA	Group IB	Group II	Group IIIA	Group IIIB
x axis	17.390	26.403	19.623(2.350)	19.663(2.457)	20.446(2.407)	20.399(2.358)	20.593(2.552)
y axis	34.720	26.481	31.409(2.548)	31.364(2.704)	29.890(2.344)	29.991(2.210)	29.564(2.702)
z axis	50.881	51.600	48.153(2.647)	48.110(2.770)	46.907(3.039)	47.081(2.876)	46.348(3.454)
Solution							
x axis			19.292(2.309)	19.205(2.316)	20.615(2.331)	⋯	⋯
y axis			30.780(2.598)	31.155(2.489)	29.197(2.241)	⋯	⋯
z axis			47.149(2.231)	47.558(1.977)	46.697(2.277)	⋯	⋯

[a]Standard deviations are given in brackets.

So, despite the fact that the very flexible crown ether molecule adopts many conformations—for the vacuum simulation over 5000 symmetry-independent conformations were sampled—they can be classified into a few groups, three maybe four. These groups will contain many different conformations that, as far as their structural aspects are concerned, show remarkable similarities.

We have done the same analysis for 18-crown-6 in solution. Figure 8 contains the distributions of the oxygen atoms, of all the recorded coordinate samples [Figs. 8(a) and 8(c)], of those samples that have a projection in the window in the lower corner of Fig. 4(a) [Fig. 8(b)], and finally of the samples that constitute group II [Fig. 8(d)]. It should be noticed that although the C_i conformation is not sampled for 18-crown-6 in cyclohexane, a considerable number of samples are close to this structure. This is confirmed by the average principle moments of inertia for the different groups given in Table III. The groups IA and IB, which are closest to the C_i structure, contain together 59.8% of all samples. Group II is not split up further into groups IIIA and IIIB.

We conclude that the structure of 18-crown-6 in cyclohexane is very similar to that of the isolated molecule.

IV. THE DIELECTRIC CONSTANT

Caswell and Suvannunt[22] have measured the dielectric properties of dilute solutions of several crown ethers in both benzene and cyclohexane. In order to calculate the mean square dipole moments from their data they have used the approximate formula of Guggenheim and Smith.

In this section we shall first derive an alternative expression for the dielectric constant of a very dilute solution, making as few approximations as possible, and clearly stating every approximation. In a second section we compare the results of our simulations with the experimental ones.

A. Theory

As is well known, the actual total mean square dipole moment of a sample depends very much on its geometry. Because the dielectric constant is a material property, i.e., is independent of the sample's geometry, the relation between the dielectric constant and the total mean square dipole moment must depend on the sample's geometry. In this paper we shall base our discussion on formulas that hold good in the case of an infinitely large sample.

Our starting point is the exact formula,[41,42]

$$\frac{(\epsilon-1)(2\epsilon+1)}{3\epsilon}=\frac{\chi^0}{\epsilon_0}, \tag{3}$$

ϵ is the relative dielectric constant of the solution, ϵ_0 is the permittivity of the vacuum, and χ^0 is the isotropic quasisusceptibility of the solution. Because we are dealing with a dilute solution, we write

$$\epsilon=\epsilon_1+\Delta\epsilon, \tag{4}$$

where ϵ_1 is the dielectric constant of the pure solvent. By expanding the left-hand side of Eq. (3), for small $\Delta\epsilon$ we get

$$\frac{(\epsilon-1)(2\epsilon+1)}{3\epsilon}=\frac{(\epsilon_1-1)(2\epsilon_1+1)}{3\epsilon_1}+\frac{2\epsilon_1^2+1}{\epsilon_1}\frac{\Delta\epsilon}{3\epsilon_1}. \tag{5}$$

In order to calculate the right-hand side of Eq. (3), we write

$$\chi^0=N_1\overline{\alpha_1^e}+N_2\overline{\alpha_2^e}+N_2\overline{\alpha_2^c}; \tag{6}$$

N_1 and N_2 are, respectively, the number of solvent and solute molecules per unit volume. $\overline{\alpha_1^e}$ is the average electric polarizability of a solvent molecule in the solution, and $\overline{\alpha_2^e}$ is defined similarly for a solute molecule. The last contribution to χ^0 results from the fluctuating dipole moments due to the conformational flexibility of the solute molecules. We call $\overline{\alpha_2^c}$ the conformational polarizability.

Next, we write

$$\overline{\alpha_1^e}=\alpha_1^e, \tag{7}$$

$$\overline{\alpha_2^e}=\alpha_2^e+\Delta\overline{\alpha_2^e}. \tag{8}$$

Equation (7) says that the electric polarizability per molecule of solvent in the solution is equal to that in the pure solvent. Equation (8) defines $\Delta\overline{\alpha_2^e}$ as the change of the electric polarizability per molecule of solute, in going from the pure solute to the solution. A nonzero value of $\Delta\overline{\alpha_2^e}$ may be found when the solute molecule in solution has a conformational distribution which differs from that in the pure liquid; the average electric polarizability will then also be different in both situations. Also, the difference between the dielectric environments of a solute molecule in solution, and one in the pure liquid, will cause a nonzero value of $\Delta\overline{\alpha_2^e}$. In view of the results of the previous section, one expects that $\overline{\alpha_2^e}$ is approximately equal to the electric polarizability of the gas phase molecule.

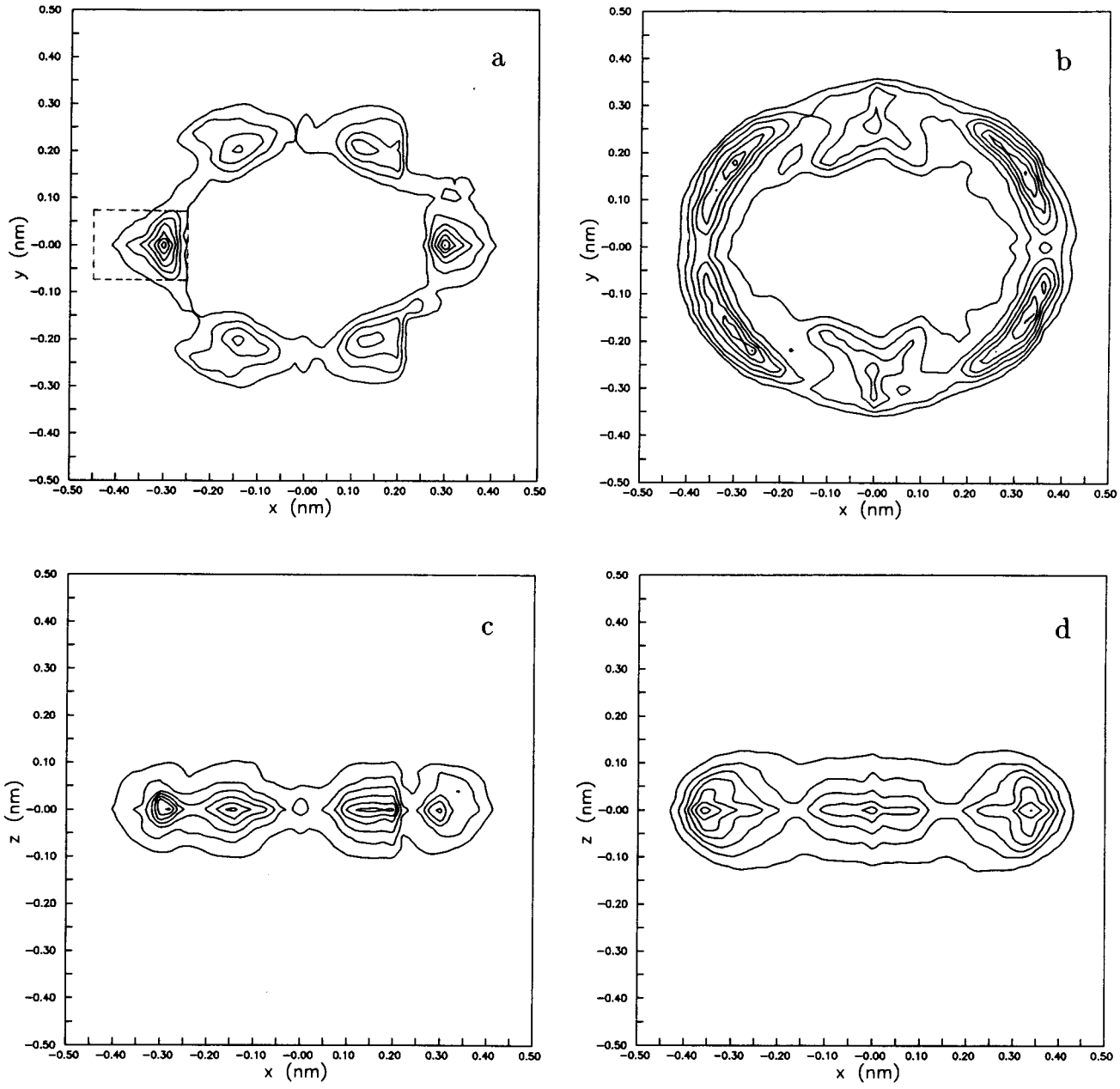

FIG. 6. Contour plots for *in vacuo* simulation I. (a) Projection of the oxygen atoms of the samples of group II (see the text) on the *xy* plane; (b) projection of the corresponding carbon atoms on the *xy* plane; (c) projection of the oxygens of (a) on the *xz* plane; (d) projection of the carbons of (b) on the *xz* plane.

We assume that the partial molar volume $\overline{v_1}$ of the solvent in the solution is equal to the molar volume v_1 of the pure solvent. The number density ρ_1 of the pure solvent is then related to N_1 and N_2 by

$$\rho_1=\frac{1}{v_1}\,(N_1\overline{v_1}+N_2\overline{v_2})=N_1+\frac{\overline{v_2}}{v_1}\,N_2. \tag{9}$$

Combining Eqs. (6)–(9) gives

$$\chi^0=\chi_1^0+\left\{\overline{\alpha_2^c}+\left(\alpha_2^e-\frac{\overline{v_2}}{v_1}\,\alpha_1^e+\Delta\,\overline{\alpha_2^e}\right)\right\}N_2. \tag{10}$$

By combining Eqs. (3), (5), and (10), we finally arrive at

$$\Delta\epsilon=\frac{3\epsilon_1^2}{2\epsilon_1^2+1}\,\frac{M_1}{M_2}\,\frac{\rho_1}{\epsilon_0}\left\{\overline{\alpha_2^c}+\left(\alpha_2^e-\frac{\overline{v_2}}{v_1}\,\alpha_1^e+\Delta\,\overline{\alpha_2^e}\right)\right\}w, \tag{11}$$

where we have made use of $N_2=w\rho_1(M_1/M_2)$, which follows for small values of w from Eq. (9), together with the expression for the weight fraction of the solute, $w=N_2M_2/(N_1M_1+N_2M_2)$. M_1 and M_2 are the molecular weights of, respectively, solvent and solute.

The magnitudes of the electric polarizabilities can be obtained by noticing that at optical frequencies $\epsilon_i=n_i^2$;[43] when introduced into Eq. (3), this yields

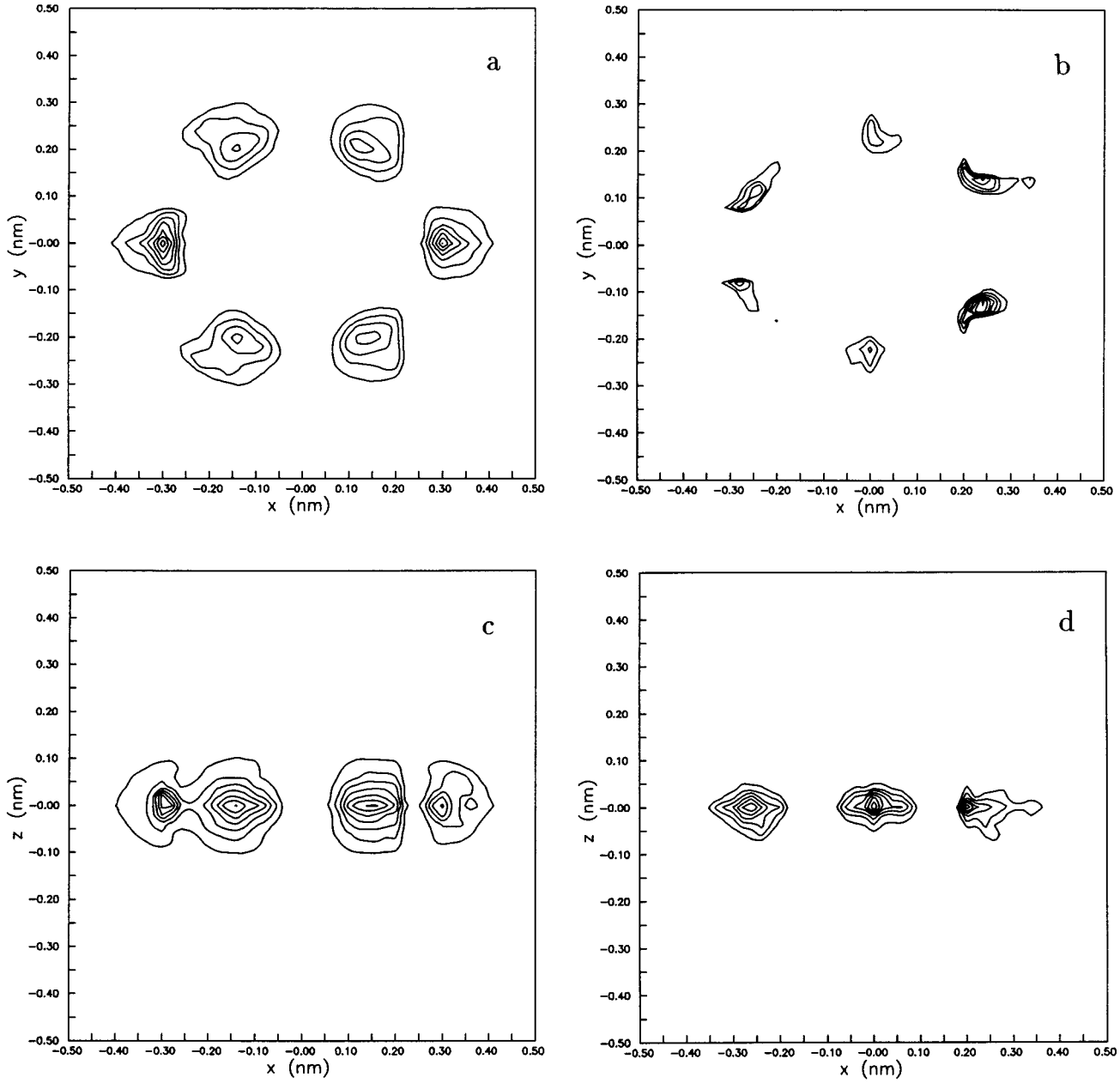

FIG. 7. Contour plots for *in vacuo* simulation I. (a) Projection of the oxygen atoms of the samples of group IIIA (see the text) on the *xy* plane; (b) projection of the oxygen atoms of the samples of group IIIB (see the text) on the *xy* plane; (c) projection of the oxygens of (a) on the *xz* plane; (d) projection of the oxygens of (b) on the *xz* plane.

$$\alpha_i^e = \frac{\epsilon_0}{\rho_i} \frac{(n_i^2-1)(2n_i^2+1)}{3n_i^2}. \tag{12}$$

The conformational polarizability is given by

$$\overline{\alpha_2^c} = \frac{\langle \mu^2 \rangle}{3kT}. \tag{13}$$

Applying Eq. (11) at high frequencies, when $\overline{\alpha_2^c}$ may be set equal to zero, yields a method to measure $\Delta\overline{\alpha_2^e}$. Once this value is know, measuring $\Delta\epsilon$ at low frequencies yields information about $\langle \mu^2 \rangle$. From now on we refer to square root of the mean square dipole moment as the average dipole moment.

B. Results

Experimentally, one measures the coefficients a and c in

$$\Delta\epsilon = aw, \tag{14}$$

$$\Delta n^2 = cw, \tag{15}$$

which according to Eq. (11), are given by

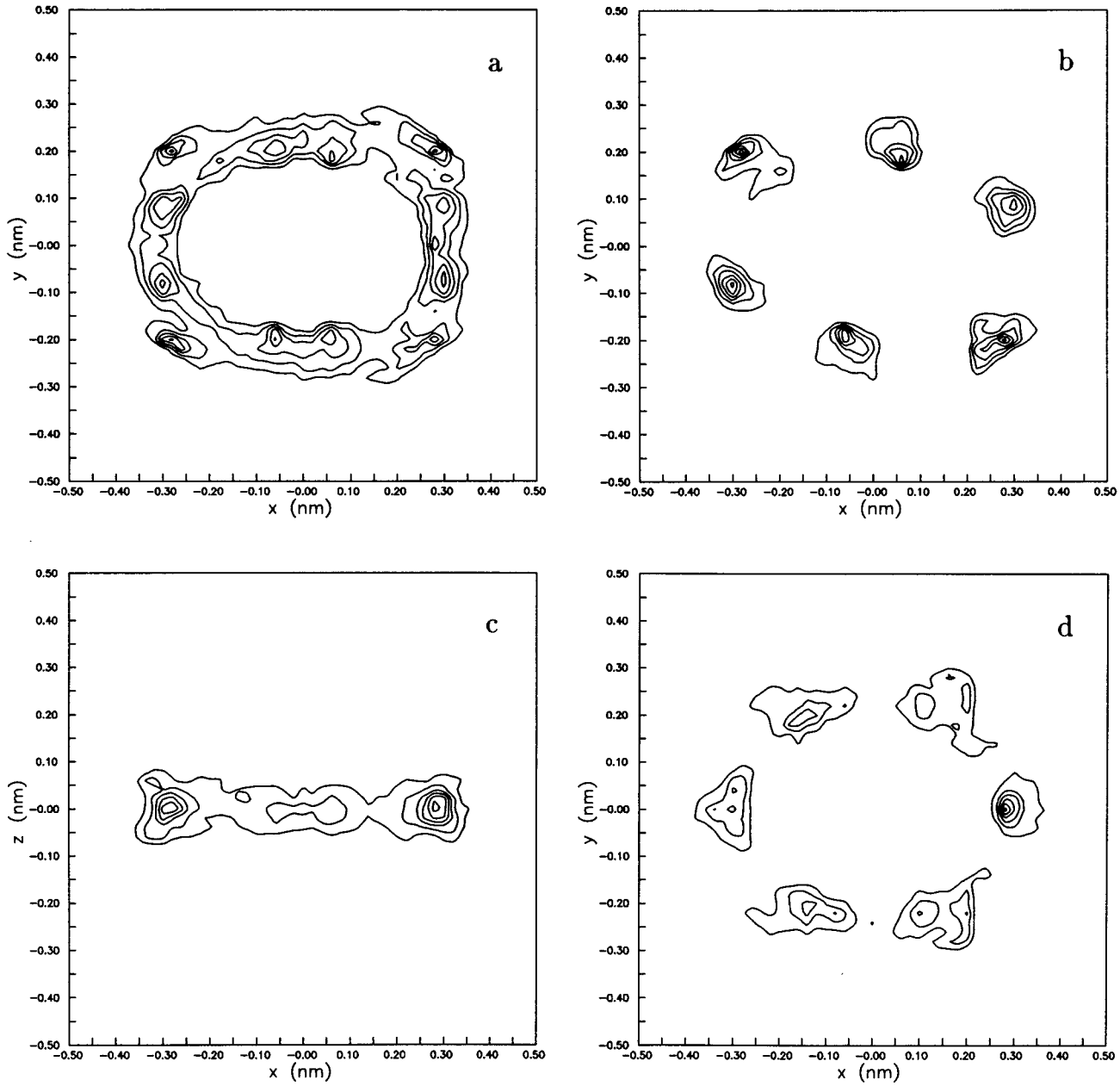

FIG. 8. Contour plots for 18-crown-6 in cyclohexane. (a) Projection of the oxygen atoms on the *xy* plane: all recorded samples; (b) projection of the oxygen atoms of group IA on the *xy* plane; (c) projection of the oxygens of (a) on the *xz* plane; (d) projection of the oxygens of group II on the *xy* plane.

$$a=\frac{3\epsilon_1^2}{2\epsilon_1^2+1}\left\{\frac{M_1}{M_2}\frac{\rho_1}{\epsilon_0}\frac{\langle\mu^2\rangle}{3kT}+\frac{2n_1^4+1}{3n_1^4}c\right\}, \tag{16}$$

$$c=\frac{3n_1^4}{2n_1^4+1}\frac{M_1}{M_2}\frac{\rho_1}{\epsilon_0}\left\{\frac{\epsilon_0}{\rho_2}\frac{(n_2^2-1)(2n_2^2+1)}{3n_2^2}-\frac{\overline{v_2}}{v_1}\frac{\epsilon_0}{\rho_1}\frac{(n_1^2-1)(2n_1^2+1)}{3n_1^2}+\Delta\overline{\alpha_2^e}\right\}. \tag{17}$$

The corresponding expressions based on the Debye equation in the Guggenheim and Smith approximation, read as

$$a=(\epsilon_1+2)^2\left\{\frac{M_1}{M_2}\frac{\rho_1}{\epsilon_0}\frac{\langle\mu^2\rangle}{27kT}+\frac{c}{(n_1^2+2)^2}\right\}, \tag{18}$$

$$c=\frac{(n_1^2+2)^2}{9}\frac{M_1}{M_2}\frac{\rho_1}{\epsilon_0}\left\{\frac{\epsilon_0}{\rho_2}\frac{n_2^2-1}{n_2^2+2}-\frac{\overline{v_2}}{v_1}\frac{\epsilon_0}{\rho_1}\frac{n_1^2-1}{n_1^2+2}+\Delta\overline{\alpha_2^e}\right\}. \tag{19}$$

Introducing the experimental values of a and c into Eq. (16), we find $\langle\mu^2\rangle=3.17$ D. This value is somewhat larger then the value of 2.76 D reported by Caswell and Suvannunt,

TABLE IV. Physicochemical constants of solvent (cyclohexane) and solute (18-crown-6).

Solvent	d_1 (g/cm^3)	0.774[a]
		0.787[b]
	n_1	1.424[a]
	ϵ_1	2.015[a]
	M_1 (g/mol)	84.162
Solute	d_2 (g/cm^3)	1.090[d]
		1.041[b]
	n_2	1.4575[d]
	M_2 (g/mol)	264.32

[a]Values at 25 °C. Taken from Ref. 27.
[b]Calculated from MD simulation.
[c]Experimental values at 50 °C. Taken from Ref. 21.

who used the formula of Guggenheim and Smith. Both values differ appreciably from the average dipole moment obtained from our simulation (see Table II). This discrepancy may be due to a deficient force field and/or to the neglect in the simulation of polarization of the solvent. Notice that, in reality, the relative dielectric constant of cyclohexane is approximately equal to 2 (see Table IV), while in our simulation it is equal to 1.

In principle, Eq. (17) can be used to calculate $\Delta\overline{\alpha_2^e}$. In order to do so, we need to know $\overline{v_2}$. From our simulation, we found $\overline{v_2}$ to be equal to 288.3 Å^3. This value differs substantially from the molecular volumes measured by Letcher *et al.*,[44,45] who reported volumes in the range from 364.0 Å^3 in the very polar acetonitrile to 390.7 Å^3 in the nonpolar CCl_4. The molecular volume of the crown in CCl_4 is significantly smaller than the value for pure liquid 18-crown-6, but much larger than the value we calculated for cyclohexane. To have at least a partial check on this value, we also calculated the molecular volume of 18-crown-6 in its liquid state. Our value of 424.0 Å^3 compares rather well with the experimental volume of 404.9 Å^3 (see Table V and Sec. II).

Because of the remaining uncertainty about the value of $\overline{v}_2$, we have estimated $\rho_2\Delta\overline{\alpha_2^e}/\epsilon_0$ [see Eq. (12)] from Eq. (17) using three different values of $\overline{v_2}$. In case $\overline{v_2}=v_2$ (approximation A), we find $\rho_2\Delta\overline{\alpha_2^e}/\epsilon_0=-0.02$, where ρ_2 is the number density of the pure liquid. If we take for $\overline{v_2}$ the result obtained from our simulation, we get $\rho_2\Delta\overline{\alpha_2^e}/\epsilon_0=-0.27$. With the value of Letcher *et al.* obtained for the apolar CCl_4 (approximation B), we get $\rho_2\Delta\overline{\alpha_2^e}/\epsilon_0=-0.05$. Clearly, the value of $\rho_2\Delta\overline{\alpha_2^e}/\epsilon_0$ is very sensitive to the value of $\overline{v_2}$ [see Table V. In Table V, also, the values of $\rho_2\Delta\overline{\alpha_2^e}/\epsilon_0$ calculated from Eq. (19) are given]. The above values of $\rho_2\Delta\overline{\alpha_2^e}/\epsilon_0$ should be compared with $\rho_2\alpha_2^e/\epsilon_0$, which is equal to 0.93. Assuming that $\overline{v_2}$ in cyclohexane will be close to that in CCl_4, the correction $\Delta\overline{\alpha_2^e}$ is seen to be rather small. This seems reasonable in view of the absence of conjugated unsaturated bonds in the molecule.

V. DYNAMICAL PROPERTIES

We have seen in Sec. III that the conformational statistics of the crown ether molecule in vacuum and in cyclohexane are very much alike. In this section we investigate the dynamical properties of the crown ether molecule, again once in vacuum (potential model I) and once dissolved in cyclohexane. We shall do this by looking at different time correlation functions of the molecular dipole.

In vacuum the decay of the dipole–dipole correlation function is caused by intramolecular motions, which in our case are as violent as to include not only harmonic vibrations, but also conformational transitions. In solution, the decay of the dipole–dipole time correlation function is caused by intramolecular motions, as well as rotations of the whole molecule. In order to separate intramolecular motions from rotations, we define a molecule-fixed reference frame, whose xy plane coincides with the least squares plane of the D_3d structure. The axes are chosen, such that the projection of one of the oxygen atoms on this plane is situated on the x axis. The origin of the reference frame coincides with the center of mass of the molecule. Next, we take those normal mode coordinates of the D_3d structure having nonzero frequency, to describe the conformation of the molecule. Every conformation of the molecule may then be specified by giving the center of mass, the Euler angles $\omega=\{\alpha,\beta,\gamma\}$ of the molecule-fixed frame with respect to the laboratory frame, and the internal coordinates $Q^{3N-6}=\{Q_1,Q_2,\ldots,Q_{3N-6}\}$, where N is the number of atoms in the molecule. Instead of giving ω, one may also give the rotation matrix, whose columns contain the coordinates of the molecule-fixed coordinate axes with respect to the laboratory frame. Details of the algorithm used to calculate these parameters for a given set of atomic positions will be given elsewhere.[46]

Characteristics of the simulations described below can be found in Table I.

In Figs. 10(a) and 10(b) are given the correlation functions $\langle\mu_\alpha(0)\mu_\alpha(t)\rangle_Q$ for the vacuum and the solution, re-

TABLE V. Several results from simulations and experiment.

			$\rho_2\Delta\overline{\alpha_2^e}/\epsilon_0$		$\langle\mu^2\rangle^{1/2}$	
	v_2[a]	$\overline{v}_2$[a]	Kirkwood[b]	Guggenheim[c]	Kirkwood	Guggenheim
Simulation	404.9	288.3	−0.27	−0.05	2.04[d]	
Approximation A	404.9	404.9	−0.02	0.02	⋯	⋯
Approximation B	404.9	390.7	−0.05	0.01	⋯	⋯
Experiment	404.9	⋯	⋯		3.17[d]	2.76[d]

[a]In Å^3.
[b]Calculated from Eq. (17). Compare with $\rho_2\alpha_2^e/\epsilon_0=0.93$.
[c]Calculated from Eq. (19). Compare with $\rho_2\alpha_2^e/\epsilon_0=0.27$.
[d]In Debye.

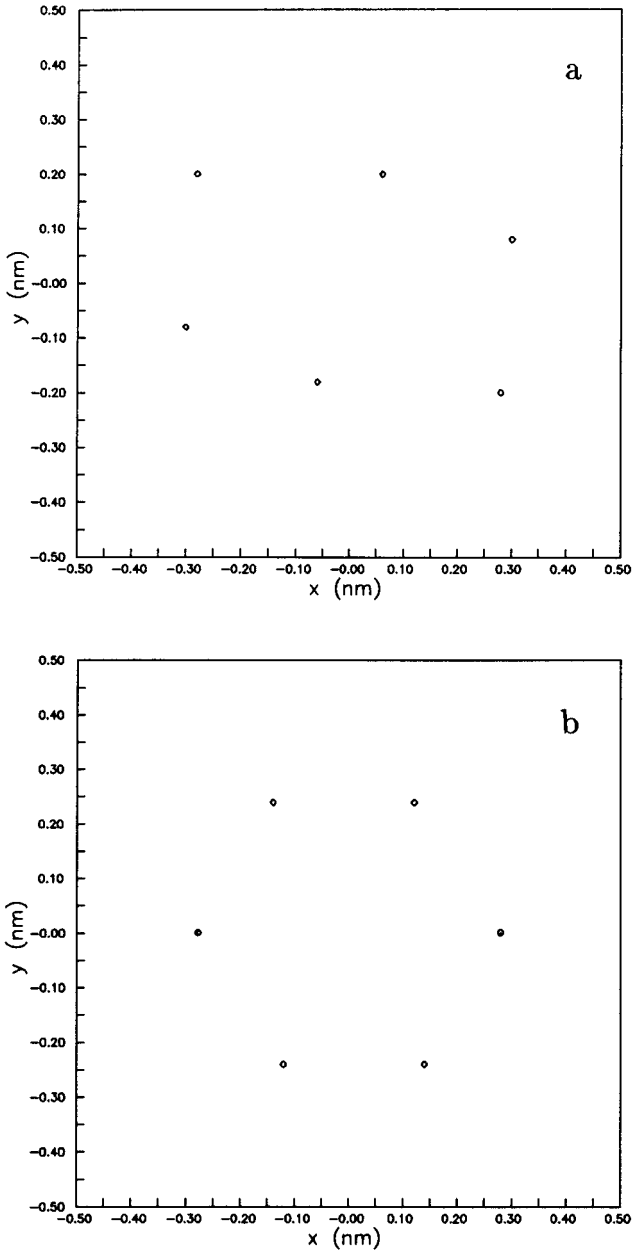

FIG. 9. Projections of the oxygen atoms on the xy plane formed by the principal axes of inertia for (a) minimized C_i conformation; (b) minimized D_3d conformation.

spectively, where the components of the dipole moments are taken with respect to the molecule-fixed frame. It is seen that in solution these functions decay exponentially, with correlation times $\tau_x=105.5$ ps, $\tau_y=30.3$ ps, and $\tau_z=34.8$ ps. The same does not hold in vacuum. The reason for this is that the number of degrees of freedom is too small to produce exponential decay; in solution, however, the solvent friction provides a second mechanism to get this result. In accordance with the definition of the molecule-fixed frame, the x and y components of the dipole moment behave rather similar in the vacuum simulation, while the z component behaves different. Surprisingly, in the solution it is the x component that behaves deviant.

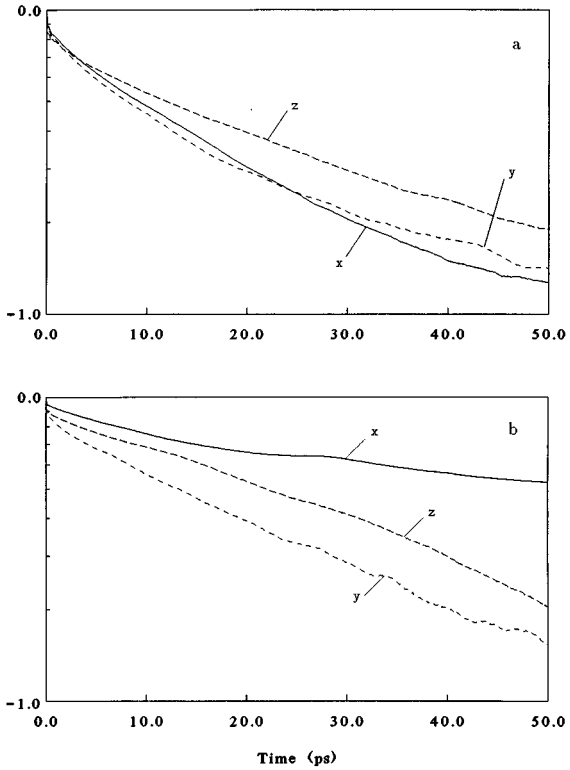

FIG. 10. Normalized correlation functions of the components of the dipole moment: $\langle\mu_\alpha(0)\mu_\alpha(t)\rangle/\langle\mu_\alpha(0)\mu_\alpha(0)\rangle$, $\alpha=x,y,z$. (a) For the vacuum simulation; (b) for the solution. Rotation was eliminated from the system (the y axis on the log scale).

In Fig. 11 the correlation functions $\langle\boldsymbol{\mu}(0)\cdot\boldsymbol{\mu}(t)\rangle_Q=\Sigma_\alpha\langle\mu_\alpha(0)\mu_\alpha(t)\rangle_Q$ are given, both for the vacuum and the solution. Apart from a small slowing down of the decay, it is difficult to identify the influence of the solvent on the dipole–dipole time correlation function. To this end, we we have Fourier transformed these functions and plotted the results in Figs. 12(a) and 12(b). In order to calculate the Fourier transform of $\langle\boldsymbol{\mu}(0)\cdot\boldsymbol{\mu}(t)\rangle_Q$, we have, for the liquid, first fitted the part between 1.0 and 10.0 ps to an exponential function, and subtracted this from the calcu-

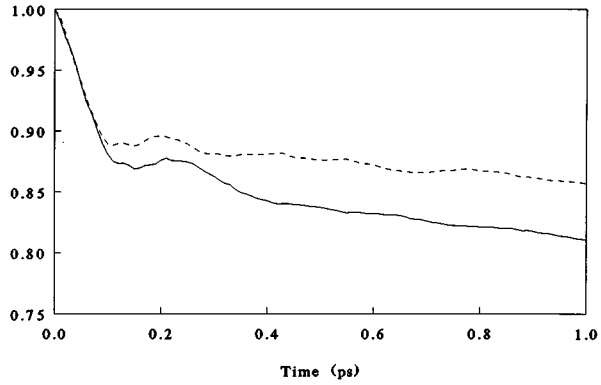

FIG. 11. Normalized correlation functions of the dipole moment vector for the gas phase simulation (solid line) and the solution (dashed line). For this figure, properties were sampled every five dynamics steps. Notice that the functions are shown for the time span 0–1 ps.

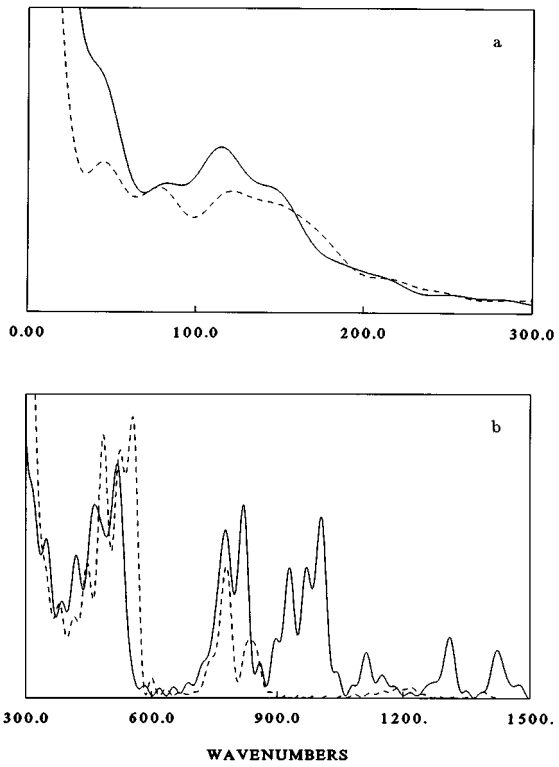

FIG. 12. Fourier transforms of the dipole correlation functions of Fig. 11. (a) Showing the low frequencies; (b) higher frequencies. Solid lines corresponds to the vacuum simulation, the dashed lines to the solution.

lated correlation function. The result was a function that was nearly zero for all times larger than 1.0 ps. Fourier transformation of this function and adding the analytic transform of the exponential part yielded a curve that was almost equal to the dotted line in Fig. 12(a), which was obtained by simply transforming the curve of Fig. 11. As expected, at low wave numbers the solvent friction has somewhat smoothed the spectrum. We notice that the absence of frequencies above 900 cm^{-1} in the case of the solvent simulation is due to the fact that in that case all bonds were constrained to their equilibrium values.

In Fig. 13 the correlation functions $\langle \hat{e}_\alpha(0)\cdot\hat{e}_\alpha(t)\rangle_\omega$ of

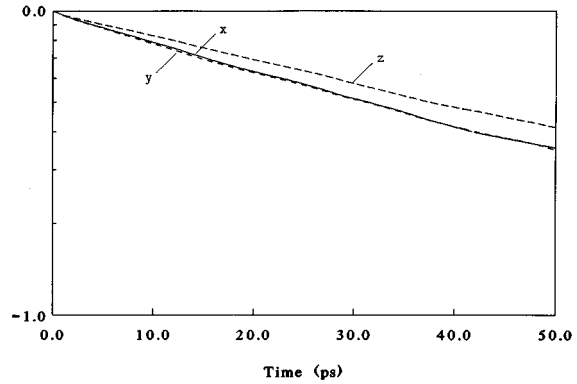

FIG. 13. Normalized correlation functions of the coordinate axes $\hat{e}_\alpha$, $\alpha=x,y,z$ of the molecule-fixed frame.

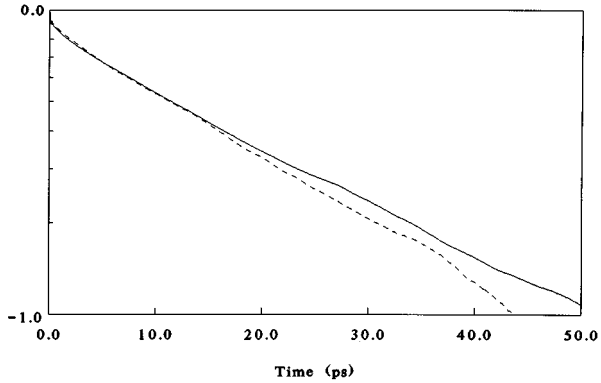

FIG. 14. Normalized correlation functions of the dipole moment vector. The solid line is the correlation function calculated according to Eq. (20), and is the product of the components shown in Figs. 10(b) and 13. The dashed line is the correlation function calculated from the dipole moments with respect to the laboratory frame of axes (the y axis on the log scale).

the coordinate axes $\hat{e}_\alpha$ of the molecule-fixed frame are plotted for the crown ether in solution. We see that these functions decay like perfect exponentials. The two in-plane axes behave equivalently while the perpendicular axis behaves slightly slower; the decay times are $\tau_x=48.3$ ps, $\tau_y=49.0$ ps, and $\tau_z=56.5$ ps.

Finally, we expect that the rotations and the intramolecular motions are decoupled to a large extent. If this holds, we may calculate $\langle \boldsymbol{\mu}(0)\cdot\boldsymbol{\mu}(t)\rangle$, with the dipole taken in the laboratory frame, according to

$$\langle \boldsymbol{\mu}(0)\cdot\boldsymbol{\mu}(t)\rangle = \sum_\alpha \sum_\beta \langle \mu_\alpha(0)\mu_\beta(t)\rangle_Q \langle \hat{e}_\alpha(0)\cdot\hat{e}_\beta(t)\rangle_\omega$$

$$= \sum_\alpha \langle \mu_\alpha(0)\mu_\alpha(t)\rangle_Q \langle \hat{e}_\alpha(0)\cdot\hat{e}_\alpha(t)\rangle_\omega . \tag{20}$$

Notice that $\langle \hat{e}_\alpha(0)\cdot\hat{e}_\beta(t)\rangle_\omega$ is diagonal at $t=0$, and will certainly be zero for large values of t. We have assumed in Eq. (20) that $\langle \hat{e}_\alpha(0)\cdot\hat{e}_\beta(t)\rangle_\omega$ will be diagonal at all times at which $\langle \mu_\alpha(0)\mu_\beta(t)\rangle_Q$ differs from zero appreciably. In Fig. 14 we have plotted $\langle \boldsymbol{\mu}(0)\cdot\boldsymbol{\mu}(t)\rangle$, once calculated from the simulation run, and once according to Eq. (20). We see that the agreement is fairly good, and that indeed internal motions and rotations are decoupled. We stress that there is no *a priori* reason for this to be so, because the fluctuating inertia tensor resulting from internal motion might have coupled both types of motion.

VI. DISCUSSION AND CONCLUSIONS

In this paper we have studied the dipole moment of 18-crown-6. In practice, the dipole moment of this molecule, which cannot be obtained with sufficient concentrations in the gaseous state, is determined from the dielectric constants of dilute solutions in nonpolar solvents. For a flexible molecule like 18-crown-6, it is assumed that the conformational statistics are, to a large extent, the same in the apolar solvent and in the gas phase.

We have performed very long molecular dynamic simulations of 18-crown-6 *in vacuo*, and in cyclohexane and made an extensive comparison of the structural characteristics of the crown ether molecule in both cases.

A. Structural properties

During the two *in vacuo* simulations that we have done, the C_i conformation was most frequently sampled. Previous experimental[2,3,6,47] and molecular mechanics studies[11,48–51] suggest that the C_i structure and the D_3d structure are among the lowest-energy conformers of uncomplexed 18-crown-6. With the first potential model the D_3d conformation was sampled with rather low frequency, while it was not observed at all with the second model. This is consistent with the fact that the D_3d conformer has unfavorable intramolecular dipole interactions in a low dielectric environment. Another reason for not sampling the D_3d structure may be related to its low degeneracy. A nonsymmetrical conformation (C_1 symmetry) has six nonequivalent permutations that produce the same conformation. A high-symmetrical structure like the D_3d conformer has only one nonequivalent permutation. This symmetry related degeneracy makes the possibility of finding a conformation like the D_3d structure six times smaller than a nonsymmetrical conformation.

In the solution, both the C_i and the D_3d conformations were not sampled, although on the basis of the distribution of the dihedral angles the crown ether molecule may be viewed to fluctuate around the C_i conformation. This is consistent with the fact that 18-crown-6 crystallizes in the C_i structure from apolar solvents. The distribution for the solution was found to be almost identical to that for *in vacuo* simulation I.

Besides looking at the sampled conformations and the distributions of the dihedral angles, we have characterized the average shape of the crown ether by means of the distribution of the mass within the molecule by projecting the positions of the atoms on the planes defined by the eigenvectors of the inertia tensor. We have applied this procedure to the sampled coordinate sets from *in vacuo* simulation I and to the 18-crown-6 molecule in the cyclohexane solution. The results for both simulations showed the same characteristics. From the projections of the atom positions on the different planes, we clearly recognized that for both systems the average shape of the crown ether is elongated like the elliptically shaped C_i conformation. Moreover, we were able to divide, for both simulations, the coordinate sets into a small number of groups. The samples within such a group show the same structural features. Many samples were found to resemble the C_i structure, although they could not be characterized as such on the basis of the values of their dihedral angles. This resemblence with the C_i conformer is confirmed by the average values of the principal moments of inertia given in Table III. These findings are in agreement with the results from the distributions of the torsion angles.

From the calculations we have done with potential model I, we arrive to the conclusion that conformational statistics is actually all but the same in a nonpolar solvent and in the gas phase.

B. Dipole moments

In polar media, solute–solvent interactions may change this population of conformations. Troxler and Wipff, for instance, who used nearly the same force field for the crown ether molecule as we did in *in vacuo* simulation II, found that the C_i and the D_3d structures are the highest populated conformations in acetonitrile. They observed that the lowest interaction energies between solvent and solute often corresponded with a nearly zero dipole moment for the crown ether. This explains the difference between the dipole moment calculated from the acetonitrile solution (2.14 D), and the value we found from *in vacuo* simulation II (2.39 D). In case of the isolated crown ether, the conformations will be populated according to their Boltzmann factors, and the average structure will be more unsymmetrical.

Wipff *et al.*,[11] and later Weiner *et al.*,[48] reported a C_1' conformation they had constructed and refined with molecular mechanics. This low-energy structure is a combination of the C_i and the D_3d conformation. They stated that this C_1' conformer, with a calculated dipole moment of 1.9 D, could contribute significantly to the average solution properties of 18-crown-6. This conformation was the second most frequently sampled structure (freq. 3.50%) from *in vacuo* simulation I. For this conformation we calculated an average dipole moment of 1.77 D. In case of *in vacuo* simulation II, this conformer appeared as number 12 on the frequency list, with an average dipole moment of 2.18 D. During the MD run of the cyclohexane solution, this structure was not observed, but the most frequently sampled one (freq. 10.18%), also of C_1 symmetry, shows much resemblance with the one of Wipff and Weiner. It gave an average dipole moment of 1.90 Debye.

All potential models so far yielded a dipole moment of about 2 D. Although they are consistent among each other, the predicted dipole moments are at variance with the experimental one, which has been reported to be 2.76 D.[22] Therefore we have carefully reanalyzed the formulas used to calculate the dipole moment from the measured dielectric constants. We started off from the exact equation of Kirkwood. The collective quantity χ^0 was next written as the sum of molecular contributions. This yields a definition of the effective molecular dipole moment, which in liquids having low dielectric constants may expected to be a true molecular quantity. In principle, however, this molecular quantity depends on the polarizability of the solvent. This differs from the usual interpretation of the experimental results that is based on the Debye theory. This method also yields an effective molecular dipole moment but based on the mean field approximation. Using our final expression, Eq. (16), we have calculated the dipole moment of the 18-crown-6 molecule and found a value that differs even more from the theoretical one than the previously reported result. This makes us conclude that the charges that have been used in all potential models so far may, at best, be treated as effective charges, which, in combination with the van der Waals part, yield a reasonable potential energy. In our opinion, to make further progress is to explicitly incorporate polarizabilities into the potential model. Polarizabilities may be expected to be im-

portant in 18-crown-6 because of the presence of the rather polarizable oxygen atoms. Recently, a model for water has been proposed in which the polarizability was modeled by the use of fluctuating charges.[52] This model proved to be rather successful in reproducing both the diffusion constant and the dielectric properties of water.

C. Fluctuations of the dipole moment

Finally, we have investigated the dynamics of the crown ether molecule in the gas phase and in solution by looking at the dipole–dipole time correlation functions. Rotations were removed from the systems. In cyclohexane, friction with the surrounding solvent plays an important role, leading to an exponential decay of the dipole–dipole correlation function. For the isolated molecule no exponential decay was observed. We have seen that the solvent slows down the dynamics of 18-crown-6. The correlation times determined from Fig. 10(b) are longer than possible correlation times from Fig. 10(a). For the solution we found that rotation of the molecule in the solvent and intramolecular motions of the crown ether are almost decoupled.

[1] C. J. Pedersen, J. Am. Chem. Soc. **89**, 2495 (1967).
[2] J. D. Dunitz, M. Dobler, P. Seiler, and R. P. Pihizaikerley, Acta Cryst. B **30**, 2733 (1974).
[3] J. D. Dunitz and P. Seiler, Acta Cryst. B **30**, 2739 (1974).
[4] M. Dobler, J. D. Dunitz, and P. Seiler, Acta Cryst. B **30**, 2741 (1974).
[5] C. I. Ratcliffe, J. A. Ripmeester, G. W. Buchanan, and J. K. Denike, J. Am. Chem. Soc. **114**, 3294 (1992).
[6] J. Dale, Isr. J. Chem. **20**, 3 (1980), and references cited therein.
[7] J. Dale and P. O. Kristiansen, Acta Chem. Scand. **26**, 1471 (1972).
[8] T. Yamabe, K. Hori, K. Akagi, and K. Fukui, Tetrahedron **35**, 1065 (1979).
[9] K. Hori, H. Yamabe, and T. Yamabe, Tetrahedron **39**, 67 (1983).
[10] H. Bruning and D. Feil, J. Comput. Chem. **12**, 1 (1991).
[11] G. Wipff, P. Weiner, and P. A. Kollman, J. Am. Chem. Soc. **104**, 3249 (1982).
[12] D. Gehin, P. A. Kollman, and G. Wipff, J. Am. Chem. Soc. **111**, 3011 (1989).
[13] P. D. J. Grootenhuis and P. A. Kollman, J. Am. Chem. Soc. **111**, 4046 (1989).
[14] A. E. Howard, U. C. Singh, M. Billeter, and P. A. Kollman, J. Am. Chem. Soc. **110**, 6984 (1988).
[15] Y. Sun and P. A. Kollman, J. Chem. Phys. **97**, 5108 (1992).
[16] T. P. Straatsma and J. A. McCammon, J. Chem. Phys. **91**, 3631 (1989).
[17] Y. Sun and P. A. Kollman, J. Comput. Chem. **13**, 33 (1992).
[18] F. T. H. Leuwerink, S. Harkema, W. J. Briels, and D. Feil, J. Comput. Chem. **14**, 899 (1993).
[19] J. M. Lehn, Acc. Chem. Res. **11**, 49 (1978).
[20] J. C. Hogan and R. D. Gandour, J. Am. Chem. Soc. **102**, 2865 (1980).
[21] R. Perrin, C. Decoret, G. Bertholon, and R. Lamartine, Nouv. J. Chim. **7**, 263 (1983).
[22] R. Caswell and D. S. Suvannunt, J. Heterocycl. Chem. **25**, 73 (1988).
[23] Y. L. Ha and A. K. Chakraborty, J. Phys. Chem. **95**, 10 781 (1991).
[24] W. F. van Gunsteren and H. J. C. Berendsen, Groningen Molecular Simulation Library, Groningen, The Netherlands, 1987.
[25] J. Ryckaert, G. Ciccoti, and H. J. C. Berendsen, J. Comput. Phys. **23**, 327 (1977).
[26] H. J. C. Berendsen, J. P. M. Postma, W. F. van Gunsteren, A. DiNola, and J. R. Haak, J. Chem. Phys. **81**, 3684 (1984).
[27] *Handbook of Chemistry and Physics*, 64th ed. (CRC Press, Boca Raton, FL, 1983).
[28] S. J. Weiner, P. A. Kollman, D. T. Nguyen, and D. A. Case, J. Comput. Chem. **7**, 230 (1986).
[29] U. C. Singh and P. A. Kollman, J. Comput. Chem. **5**, 129 (1984).
[30] J. G. Harris and F. H. Stillinger, J. Chem. Phys. **95**, 5953 (1991).
[31] J. D. Dunitz and P. Seiler, Acta Cryst. B **29**, 154 (1973).
[32] E. Maverick, P. Seiler, W. B. Schweizer, and J. D. Dunitz, Acta Cryst. B **36**, 615 (1980).
[33] F. H. Allen, O. Kennard, and R. Taylor, Acc. Chem. Res. **16**, 146 (1983).
[34] T. M. Fyles and R. D. Gandour, J. Inc. Phenom. **12**, 313 (1992).
[35] M. Dobler, Chimia **38**, 415 (1980).
[36] L. Troxler and G. Wipff, J. Am. Chem. Soc. **116**, 1468 (1994).
[37] J. van Eerden, W. J. Briels, S. Harkema, and D. Feil, Chem. Phys. Lett. **164**, 370 (1989).
[38] G. Ranghino, S. Romano, J. M. Lehn, and G. Wipff, J. Am. Chem. Soc. **107**, 7873 (1985).
[39] T. Kowall and A. Geiger, J. Phys. Chem. **98**, 6216 (1994).
[40] K. Fukuhara, K. Ikeda, and H. Matsuura, Spectrochim. Acta A Mol. Spectrosc. **50**, 1619 (1994).
[41] P. Madden and D. Kivelson, Adv. Chem. Phys. **LVI**, 467 (1984).
[42] J. P. Hansen and I. R. McDonald, *Theory of Simple Liquids*, 2nd ed. (Academic, New York, 1990), Chap. 12.
[43] C. J. F. Böttcher, O. C. van Belle, P. Bordewijk, and A. Rip, *Theory of Electric Polarization* (Elsevier, Amsterdam, 1973), Vols. 1 and 2.
[44] T. M. Letcher, J. J. Paul, and R. L. Kay, J. Sol. Chem. **20**, 1001 (1991).
[45] T. M. Letcher, J. D. Mercer-Chalmers, and R. L. Kay, Pure Appl. Chem. **66**, 419 (1994).
[46] W. K. den Otter and W. J. Briels (to be published).
[47] J. Dale, Tetrahedron **30**, 1683 (1974).
[48] P. K. Weiner, S. Profeta, Jr., G. Wipff, T. Havel, I. D. Kuntz, R. Langridge, and P. A. Kollman, Tetrahedron **39**, 1113 (1983).
[49] J. W. H. M. Uiterwijk, S. Harkema, B. W. van de Waal, F. Göbel, and H. T. M. Nibbeling, J. Chem. Soc., Perkin Trans. 2, 1843 (1983).
[50] M. Billeter, A. E. Howard, I. D. Kuntz, and P. A. Kollman, J. Am. Chem. Soc. **110**, 8385 (1988).
[51] M. J. Bovill, D. J. Chadwick, and I. O. Sutherland, J. Chem. Soc. Perkin Trans. **2**, 1529 (1980).
[52] S. W. Rick, S. J. Stuart, and B. J. Berne, J. Chem. Phys. **101**, 6141 (1994).